Direct observation of surface plasmon-polariton dispersion

Armando Giannattasio and William L. Barnes

School of Physics, University of Exeter, Stocker Road, Exeter, EX4 4QL, United Kingdom
a.giannattasio@exeter.ac.uk

Abstract: We describe a method to observe the directional emission of electromagnetic radiation produced by the radiative decay of surface plasmon-polaritons (SPPs) that allows the dispersion of the modes in *k*-space to be directly visualized. The method presented here opens up the possibility of characterizing the effect of a wide range of surface morphologies on SPP dispersion. As an example we show the formation of a stop-band for SPPs when the metal surface is modulated in the form of a diffraction grating.

OCIS codes: (240.6680) Surface plasmons; (260.3910) Optics of metals; (240.0310) Thin films.

References and links

1. H. Raether, *Surface Plasmons on Smooth and Rough Surfaces and on Gratings* (Springer Verlag, Berlin, 1988).
2. E. Devaux, T. W. Ebbesen, J. Weeber and A. Dereux, "Launching and decoupling surface plasmons via micro-gratings," Appl. Phys. Lett. **83**, 4936-4938 (2003).
3. W. L. Barnes, S. C. Kitson, T. W. Preist, and J. R. Sambles, "Photonic surfaces for surface-plasmon polaritons," J. Opt. Soc. Am. A **14**, 1654-1661 (1997).
4. J. B. Pendry, L. Martín-Moreno, and F. J. Garcia-Vidal, "Mimicking surface plasmons with structured surfaces," Science **305**, 847-848 (2004).
5. W. A. Murray, S. Astilean, and W. L. Barnes, "Transition from localized surface plasmon resonance to extended surface plasmon-polariton as metallic nanoparticles merge to form a periodic hole array," Phys. Rev. B **69**, 165047 (2004).
6. R. A. Depine, S. Ledesma, "Direct visualization of surface-plasmon bandgaps in the diffuse background of metallic gratings," Opt. Lett. **29**, 2216-2218 (2004).
7. J. Moreland, A. Adams, and P. K. Hansma, "Efficiency of light-emission from surface-plasmons," Phys. Rev. B **25**, 2297-2300 (1982).
8. H. J. Simon and J. K. Guha, "Directional surface plasmon scattering from silver films," Optics Communications **18**, 391-394 (1976).
9. P. R. Auvil, J. B. Ketterson, Y. Kim, and A. Kryukov, "Simple model for the observed plasmon conical radiation interference patterns in a Kretschmann configuration," Applied Optics **37**, 8448-8452 (1998).
10. Z. Liu, N. Fang, T. J. Yen, X. Zhang, "Rapid growth of evanescent wave by a silver superlens," Appl. Phys. Lett. **83**, 5184-5186 (2003).
11. N. Fang, Z. W. Liu, T. J. Yen, X. Zhang, "Regenerating evanescent waves from a silver superlens," Opt. Express **11**, 682-687 (2003), http://www.opticsexpress.org/abstract.cfm?URI=OPEX-11-7-682
12. A. Giannattasio, I. R. Hooper, and W. L. Barnes, "Transmission of light through thin silver films via surface plasmon-polaritons," Opt. Express **12**, 5881-5886 (2004), http://www.opticsexpress.org/abstract.cfm?URI=OPEX-12-24-5881
13. S. Wedge, I. R. Hooper, I. Sage, W. L. Barnes, "Light emission through a corrugated metal film: The role of cross-coupled surface plasmon polaritons," Phys. Rev. B. **69**, 245418 (2004).
14. I. Gryczynski, J. Malicka, Z. Gryczynski, and J. R. Lakowicz, "Radiative decay engineering 4. Experimental studies of surface plasmon-coupled directional emission," Anal. Biochem. **324**, 170-182 (2004).
15. S. C. Kitson, W. L. Barnes, and J. R. Sambles, "Full photonic band gap for surface modes in the visible," Phys. Rev. Lett. **77**, 2670-2673 (1996).
16. D. Hilbert and S. Cohn-Vossen, *Geometry and the Imagination* (Chelsea, New York, 1999).

1. Introduction

The nature of surface plasmon-polaritons (SPPs) [1] is strongly dependent on the morphology of the interface on which they propagate [2]. Perhaps most dramatically the formation of energy band gaps for SPP modes supported by periodic metallic structures has been

#6017 - $15.00 US Received 14 December 2004; revised 5 January 2005; accepted 7 January 2005

demonstrated [3]. Exploring the underlying physics that relates SPP properties with surface morphology continues to throw up new developments, most recently the idea that sub-wavelength structure can lead to the creation of spoof SPPs [4]. The interaction between SPPs and the morphology of the surfaces on which they propagate is often most easily understood with the aid of dispersion diagrams, however, these are difficult to obtain experimentally, usually being acquired point by point and thus time consuming to construct [5]. Thus, there is a need to develop techniques that allow the direct visualization of SPP dispersion. One such technique is based on the diffuse background emission of SPPs produced by surface roughness [6]. Here we report the use of an alternative technique by which the effect of surface/interface structure on SPP propagation can be determined and readily visualized. Moreover, the technique offers the possibility of rapid acquisition of dispersion data and may thus be of use in exploring the interaction between surface morphology and SPP properties.

Although SPPs are in general non-radiative in nature, SPP modes can under appropriate circumstances be converted to light [7]. In the past, several papers have been written on the directional emission of radiation that is observed when SPPs supported by a silver film are converted back to freely propagating light using a form of inverse prism coupling [8,9,10]. Such emitted radiation consists of a hollow cone of directionally scattered light, the axis of the cone being normal to the silver surface. The opening angle 2θ of the cone is regulated by the following equation (in-plane momentum conservation)

$$nk_0 \sin\theta = k_{spp} \tag{1}$$

where n is the index of refraction of the material through which the light propagates, k_0 is magnitude of the wavevector of the emitted light and k_{spp} is the magnitude of the wavevector of the SPPs. A simple method to observe this directional SPP-mediated radiation is described in this paper. Here we use this technique to show the marked change in dispersion of SPP modes when the surface is modulated in form of a diffracting grating. In particular, the formation and the shape of stop-bands for SPPs propagating along corrugated silver films are observed straightforwardly.

2. Experiment

The system investigated in this work consisted of an air/silver/silica interface (Fig. 1). Two structures were studied, one consisting of a planar metal film (Fig. 1(a)) and the other consisting of a metal film corrugated in the form of a diffraction grating (Fig. 1(b)). For both structures incident light is coupled to the SPP mode by scattering from surface roughness present at the silver/air interface [11]. After excitation, the SPPs can in turn be scattered by the periodic profile of the grating.

Since previous studies have demonstrated that 50 nm is approximately the optimal film thickness for SPP-mediated transmission of light through thin silver films [10,12], a silver layer of 50 nm thickness was thermally evaporated onto two 25 mm × 25 mm silica substrates (1 mm thick), one nominally flat (roughness ~1 nm) and the other having a periodic surface profile. Such periodic modulation (pitch = 380±1 nm, amplitude = 11±1 nm) was produced at the silica surface by using laser interferometry and reactive ion etching techniques [13].

Light from a He-Ne laser (λ_0 = 612 nm) was focussed directly onto the silver film, at normal incidence from the air side, by a microscope objective lens (50×) and was then scattered randomly by the natural roughness of the silver surface. Some of these scattered components had a wavevector equal to that of SPPs of the same frequency and thus allowed incident light to couple to SPP modes propagating along the metallic surface in all azimuthal directions. It is well known that the evanescent wave associated with a SPP mode decays exponentially within the metal due to absorption [1]. However, because the silver film considered in this experiment was rather thin (50 nm), the evanescent field associated with the silver/air interface was sufficiently strong at the silver/silica interface such that the SPPs had a significant probability to radiate into the silica substrate. Radiation was emitted through the

#6017 - $15.00 US Received 14 December 2004; revised 5 January 2005; accepted 7 January 2005

silica with a polar angle θ such that Eq. (1) was fulfilled. Since the SPPs were randomly generated in all directions in the plane of the metal, the emitted radiation propagating through the silica substrate consisted of a hollow cone of light with cone angle 2θ. A schematic representation of this process in *k*-space is shown in Fig. 1(a) for the case of a flat silver surface modulated only by natural roughness (no grating). The situation where SPPs are in turn scattered by a grating is illustrated in Fig. 1(b) where the scattering events are also represented in *k*-space.

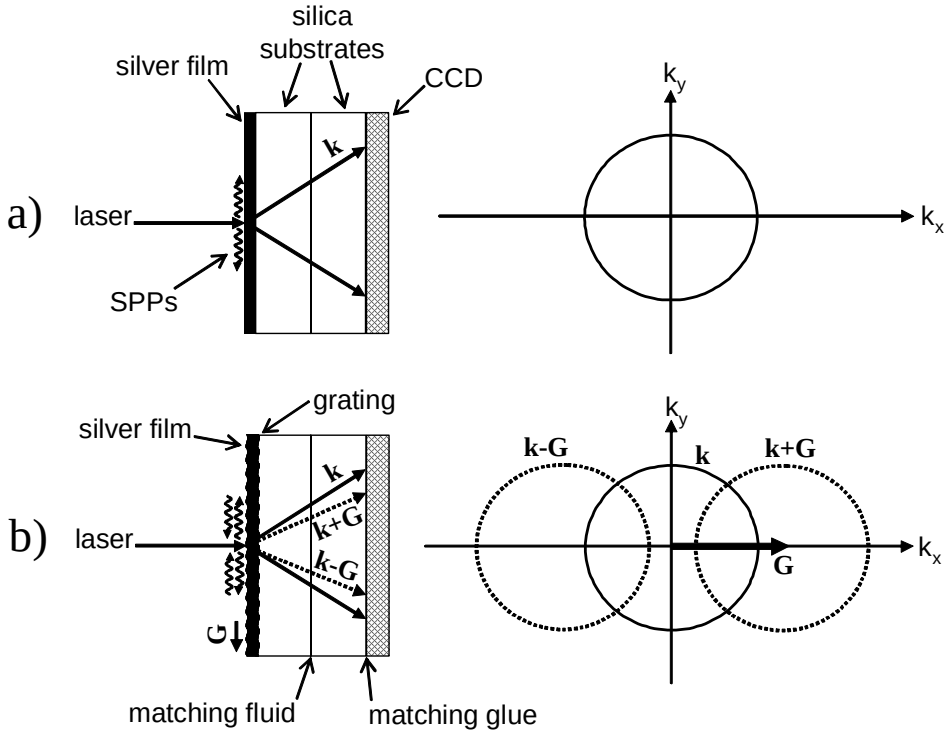

Fig. 1. Schematic of the geometry used for the experiment. a) Planar silver surface: a single cone of light is emitted into the silica substrate. b) Corrugated silver surface: the central cone (zero order scattering) is now intersected by the other cones of light due to SPPs scattered by the grating with Bragg vector $\boldsymbol{G}$.

We observed the radiation emitted into the silica substrate using a charge-coupled device (CCD). The active area of a CCD (approximately 3.4 mm×4.5 mm, 640×480 pixels), taken from a commercially available webcam, was index matched to a second silica substrate identical to that used to support the silver film. The two silica substrates were in turn index matched together, as shown in Fig. 1. With this geometry, the directional radiation that propagates in the form of a hollow cone of light through the two index-matched silica substrates is detected by the CCD which in turn is connected to a computer; the cone can thus be visualized in two-dimensions on a computer screen. The CCD used in this work was too small to detect the full circle of emitted light, as it appears schematically in Fig. 1, therefore only about a quarter (~90° arc) could be detected (the observation of a circle of emitted light was not the aim of this work since many images of this characteristic circle can be found in the literature [8,11,14]). As illustrated in Fig. 1b, it is more interesting to see whether stop-bands can be generated as a consequence of the interaction between SPPs with wavevector $\boldsymbol{k}$ (not-scattered by the grating) and other SPPs having wavevectors $\boldsymbol{k}\pm\boldsymbol{G}$ (subjected to a scattering process), with $\boldsymbol{G}$ being the Bragg vector of the grating. In fact, under certain

#6017 - $15.00 US Received 14 December 2004; revised 5 January 2005; accepted 7 January 2005

conditions, SPPs with different wavevectors can be subjected to scattering processes leading to the formation of energy band gaps [15] directly observable at the positions where the circles of Fig. 1(b) intersect each other (Fig. 2). For example, if $\boldsymbol{k_1}=\boldsymbol{k}$ and $\boldsymbol{k_2}=\boldsymbol{k}-\boldsymbol{G}$ are respectively the wavevectors of the non-scattered and scattered (by the grating) SPP modes, then

$$\boldsymbol{k_1}-\boldsymbol{k_2}=\boldsymbol{G} \tag{2}$$

which is the usual Bragg diffraction condition, with $|\boldsymbol{k_1}| = |\boldsymbol{k_2}|$. This implies that when the projection of the SPP wavevector along the *x*-axis, k_x, is such that

$$k_x = \pm m\frac{G}{2} = \pm m\frac{\pi}{a} \tag{3}$$

where *m* is an integer and *a* is the grating pitch, the SPP modes become standing waves and thus do not propagate; this produce an energy gap for SPPs. It should be possible to observe such stop-bands in *k*-space, as shown in Fig. 2.

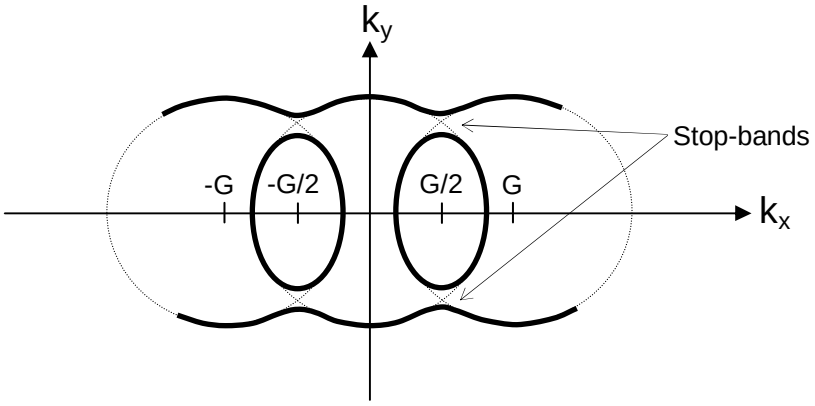

Fig. 2. Representation of the stop-bands in *k*-space. The stop-bands form at k_x=G/2 where the circles intersect each other.

3. Results

Figure 3 shows two images of *k*-space obtained with the experimental geometry shown in Fig. 1. These images were produced by using the CCD to detect the radiation emitted through the silica substrate via SPP-coupling in the two cases shown in Fig. 1(a) and Fig. 1(b) (in the absence (a) and in the presence (b) of a grating). The bright arc that appears in Fig. 3(a) is part of the conical radiation emitted following the decay of those SPPs which were scattered by the rough surface of the silver. This cone of light is schematically represented by the circle centred on the *k*-space origin shown in Fig. 1(a).

Results for the case of the sample with periodic surface modulation are shown in Fig. 3(b). In this figure, the brighter arc again represents the zero-order emitted radiation (the same as in Fig. 3(a) observed in the absence of a grating), which corresponds to the central circle in Fig. 2. Part of the circle formed by light emitted by those SPPs excited at the silver/silica interface and subjected to a first order scattering is also visible in Fig. 3(b), although this is a less efficient process than the zero order.

The stop-band arising at k_x=*G*/2 due to the interaction of the scattered and non-scattered SPPs is clearly visible in Fig. 3(b), where the two circles generated by the (scattered and non-scattered) SPPs intersect each other. However, since *k*-space is projected into the plane of the CCD and not into a hemispherical screen (see Fig. 4), the circle generated by the first order scattered radiation is deformed, as this is given by the intersection of a cone with a plane and originates either an elliptic or a parabolic curve [16]. The equation of such curve in the *xy* plane of the screen is of the form:

#6017 - $15.00 US Received 14 December 2004; revised 5 January 2005; accepted 7 January 2005

$$x^2 = y^2(\tan^2\theta\sin^2\gamma - \cos^2\gamma) + 2yL(\tan^2\theta + 1)\sin\gamma\cos\gamma + L^2(\tan^2\theta\cos^2\gamma - \sin^2\gamma) \qquad (4)$$

where L is the separation between the silver film and the CCD, θ is the angle given by Equation (1) and γ is the angle between the normal to the sample surface and the axis of the scattered cone. If γ=0, the axis of the emitted cone of light is perpendicular to the metallic surface (zero order) and such radiation appears on the screen like a regular circle of radius $L\tan(\theta)$.

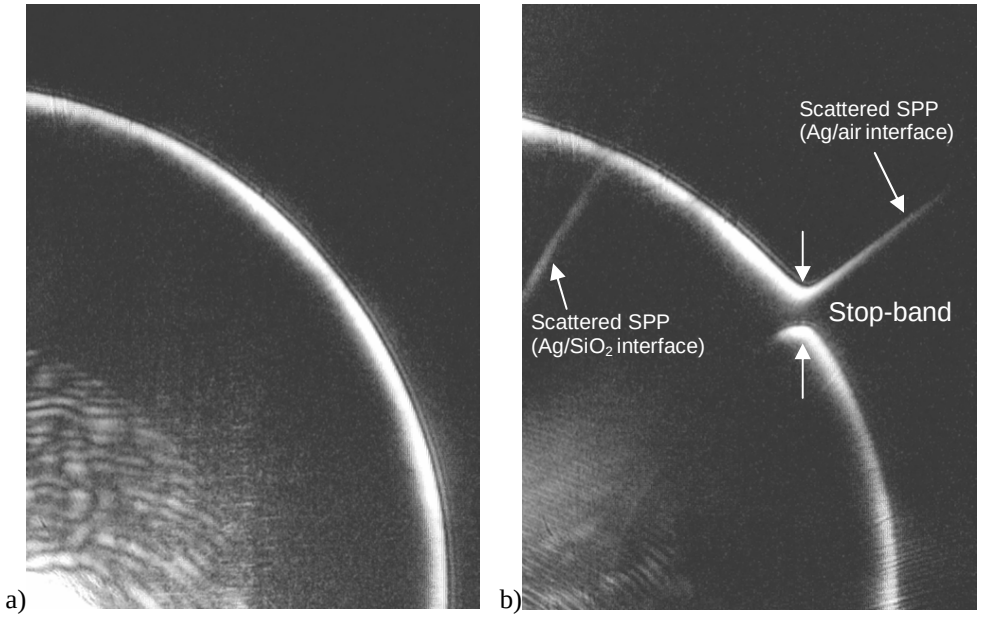

Fig. 3. Direct image of the conical radiation in *k*-space as recorded by the CCD. a) Planar control sample. b) The presence of a grating introduces new scattering events. As a result, a stop-band opens up at the intersection of the two circles, one generated by non-scattered SPPs (much brighter) and the other resulting from scattering processes (faint). The extra line that is noted crossing the circle, at the top-left, is due to SPPs excited at the silver/silica interface, but these do not produce a visible stop-band.

If the conical radiation had been collected by using a hemispherical CCD device, then the resulting image would have been very similar to that drawn in Fig. 1(b) which shows a series of regular circles. However, in this work, the coordinates *xy* used in Eq. (4) to describe the curve observed on the screen can be linked to the actual components k_x and k_y of the wavevector of SPPs by defining the angles (see Fig. 5):

$$\alpha = \arctan\frac{y}{x} \quad ; \quad \beta = \arctan\frac{\sqrt{x^2 + y^2}}{L} \qquad (5)$$

such that

$$k_x = nk_0 \sin\beta\cos\alpha \pm mG \qquad (6)$$

$$k_y = nk_0 \sin\beta\sin\alpha \qquad (7)$$

#6017 - $15.00 US Received 14 December 2004; revised 5 January 2005; accepted 7 January 2005

where m is an integer, n is the index of refraction of silica, G is the Bragg vector of the grating and k_0 is the magnitude of the wavevector of scattered light.

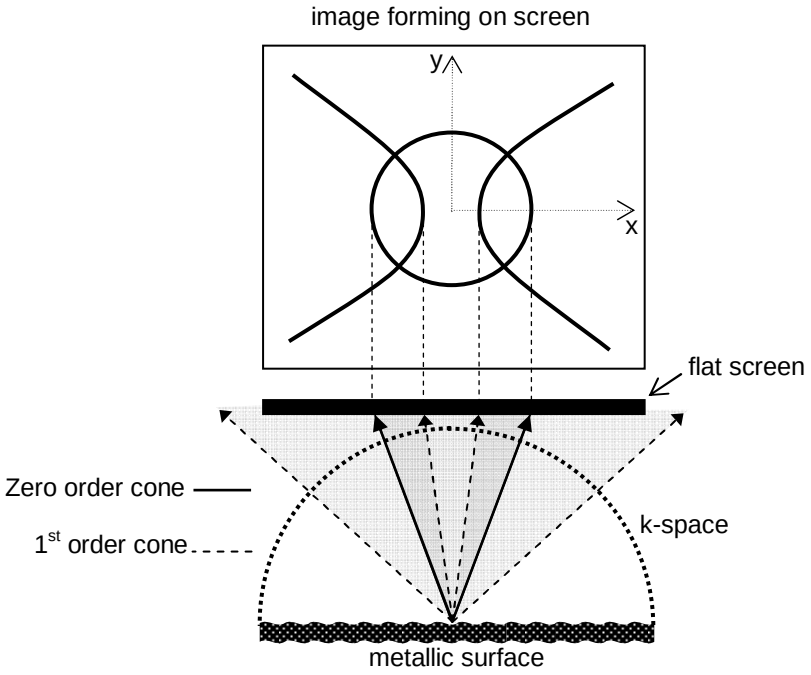

Fig. 4. The conical radiation due to the different SPP scattering processes is projected into a flat screen (CCD) and thus the resulting image in *k*-space is distorted, as shown in this schematic illustration. The image on the screen would have been similar to that drawn in Fig. 1b if the radiation had been projected onto a hemispherical screen.

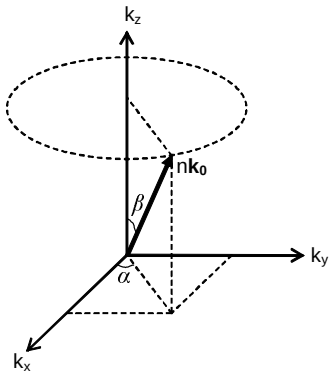

Fig. 5.Geometry and angles chosen to define the wavevector of the scattered light, $n\mathbf{k_0}$, in *k*-space.

#6017 - $15.00 US Received 14 December 2004; revised 5 January 2005; accepted 7 January 2005

The amplitude and shape of the stop-band for SPP modes shown in Fig. 3 depends primarily on the amplitude of the grating. Figure 6 shows different band gaps obtained using a 50 nm silver film evaporated on silica gratings with different amplitudes (5-40 nm).

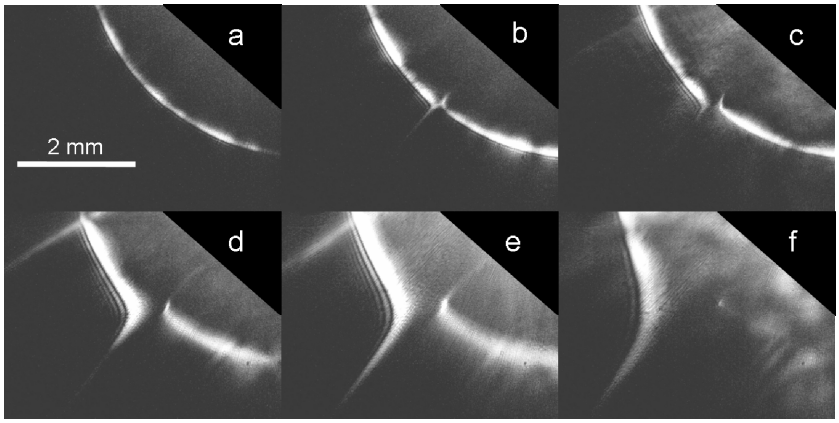

Fig. 6. SPP band gaps forming in 50 nm thin metallic films deposited on a grating. Picture (a) shows again the case where the grating is not present. The other pictures refer to gratings with amplitude of approximately (b) 5 nm, (c) 10nm, (d) 20 nm, (e) 30 nm and (f) 40 nm.

4. Conclusions

The results reported above provide clear evidence that the technique described here can be used as a way to rapidly evaluate the effect of surface morphology on the propagation of surface plasmon-polaritons. It should thus be a valuable tool in the quest for a better understanding of the correlation between surface morphology and SPP properties.

Acknowledgments

The authors thank Dr. I. R. Hooper and Dr. S. Wedge at the University of Exeter for many valuable discussions and for producing the silica gratings used in this work.

The support of the EC through funding the project “Surface Plasmon Photonics” FP6 NMP4-CT-2003-505699 is gratefully acknowledged.

#6017 - $15.00 US Received 14 December 2004; revised 5 January 2005; accepted 7 January 2005